Chemistry Europe
European Chemical Societies Publishing

WILEY VCH

Excellence in Chemistry Research

Announcing our new flagship journal

- Gold Open Access
- Publishing charges waived
- Preprints welcome
- Edited by active scientists

Meet the Editors of *ChemistryEurope*

Luisa De Cola
Università degli Studi di Milano Statale, Italy

Ive Hermans
University of Wisconsin-Madison, USA

Ken Tanaka
Tokyo Institute of Technology, Japan

Chemistry
A European
Journal

Chemistry Europe
European Chemical Societies Publishing

Accepted Article

Title: Platinum(IV)-Gold(I) Agents with Promising Anticancer Activity. Selected Studies in 2D and 3D Triple Negative Breast Cancer Models

Authors: Javier E. Lopez-Hernandez, Nazia Nayeem, José P. Cerón-Carrasco, Afruja lAhad, Aiman Hafeed, Ignacio E. León, and Maria Contel

To be cited as: *Chem. Eur. J.* **2023**, e202302045

Link to VoR: https://doi.org/10.1002/chem.202302045

WILEY VCH

10.1002/chem.202302045

WILEY-VCH

RESEARCH ARTICLE

Platinum(IV)-Gold(I) Agents with Promising Anticancer Activity. Selected Studies in 2D and 3D Triple Negative Breast Cancer Models

Javier E. López-Hernández,[a,b] Nazia Nayeem,[a,b] José P. Cerón-Carrasco,[c] Afruja Ahad,[a,b,d] Aiman Hafeez,[a] Ignacio E. León,[e] and Maria Contel*[a,b]

[a] J.E. López-Hernández, N. Nayeem, A. Ahad, A. Hafeez, Prof. M. Contel
Department of Chemistry and Brooklyn College Cancer Center
Brooklyn College, The City University of New York
Brooklyn, NY, 11210(USA)
E-mail: mariacontel@brooklyn.cuny.edu
[b] J.E. López-Hernández, N. Nayeem, A. Ahad, Prof. M. Contel
Biology, Chemistry and Biochemistry PhD Programs, The Graduate Center,
The City University of New York
New York, NY, 10016(USA)
[c] Dr. J.P. Cerón-Carrasco
Centro Universitario de la Defensa, Universidad Politécnica de Cartagena,
C/Coronel López Peña s/n, Base Aérea de San Javier, Santiago de la Ribera, 30720 Murcia, Spain
[d] A. Ahad
Radiology, Molecular Pharmacology Program, and
Radiochemistry and Molecular Imaging Probes Core
Memorial Sloan Kettering Cancer Center, New York, NY 11065(USA)
[e] Dr. I.E. León
Centro de Química Inorgánica, CEQUINOR (CCT-CONICET La Plata, Asociado a CIC)
Departamento de Química, Facultad de Ciencias Exactas, Universidad Nacional de La Plata
Blvd. 120 N°1465, La Plata 1900, Argentina

Supporting information for this article is given via a link at the end of the document

Abstract: New heterometallic binuclear and trinuclear platinum(IV)-gold(I) compounds of the type $[Pt(L)_nCl_2(OH)\{(OOC\text{-}4\text{-}C_6H_4\text{-}PPh_2)AuCl\}_x]$ (L=NH_3, n = 2; x = 1,2; L = diaminocyclohexane, DACH, n = 1; x = 2) are described. These compounds are cytotoxic and selective against a small panel of renal, bladder, ovarian and breast cancer cell lines. We selected a trinuclear $PtAu_2$ compound containing the Pt(IV) core based on oxaliplatin, to further investigate its cell death pathway, cell and organelle uptake and anticancer effects against triple negative breast cancer (TNBC) MDA-MB-231 cell line. This compound induces apoptosis and accumulates mainly in the nucleus and mitochondria. It also exerts remarkable antimigratory and antiangiogenic properties, and has a potent cytotoxic effect against TNBC 3D spheroids. Trinuclear compounds do not seem to display relevant interactions with calf thymus (CT) DNA and plasmid (pBR322) even in the presence of reducing agents, but inhibit pro-angiogenic enzyme thioredoxin reductase (TrxR) in TNBC cells.

Introduction

Cancer chemotherapy is limited by intrinsic and acquired resistance of tumors to treatment, and lack of selectivity that leads to off-site toxicity and serious side-effects.[1] Despite multiple advances in cancer precision medicine and targeted therapies,[2] cancer chemotherapy alone or in combination with other types of therapy and surgery, is still the standard of care for most patients. Platinum(II)-based drugs such as FDA-approved cisplatin, carboplatin, and oxaliplatin (Fig. 1 **a**-**c**) are widely used as chemotherapeutics to treat different solid tumors.[3] These drugs have a limited spectrum of activity and thus they are more efficacious against testicular, colorectal, gastric, head and neck, lung, bladder, ovary, and endometrial cancers, but are still limited by lack of selectivity and appearance of resistance.[4] Over the past 15 years there has been a considerable effort in developing non-conventional Pt(II) drugs,[5] understanding resistance and transport mechanisms,[6] and improving the pharmacological profile and bioavailability of these drugs by encapsulation in nanocarriers or binding to targeting vectors.[7-9] Results from these studies and recent clinical trials underscore the fact that Pt drugs (alone or in combination) remain the standard of care for some cancers like ovarian cancer in the near future.[10,11]

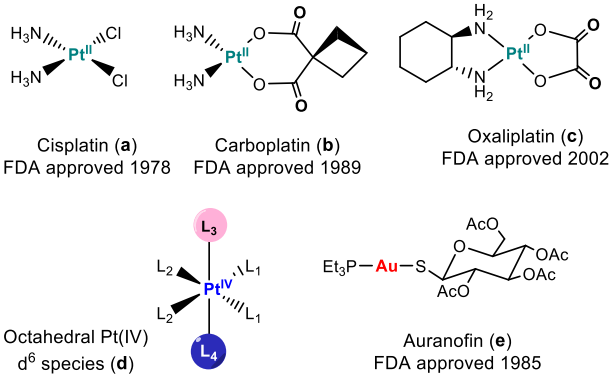

Figure 1. FDA-approved Pt(II)-based square-planar drugs for the treatment of cancer (**a**-**c**). Pt(IV) octahedral compound (**d**), and Au(I) derivative (**e**) approved for the treatment of rheumatoid arthritis.

Pt(IV) compounds are an attractive approach to improve stability and bioavailability of platinum drugs. Less labile d^6 Pt^{4+} octahedral compounds are more stable in biological media and can be

10.1002/chem.202302045

reduced by different agents to square-planar d^8 Pt(II) in the cellular milieu of tumor cells.[12-17] The octahedral geometry of Pt(IV) allows for attachment of two extra ligands in the axial position (Fig. 1 **d**) which can then get released after reduction. The solubility, activity, and selectivity of the parent Pt(II) compounds may be improved by choosing moieties with well-known anticancer effects and/or targeting vectors.

There are examples of Pt(IV) compounds containing FDA-approved Pt and bioactive ligands such biotin, glucose arginylglycylaspartic acid (RGD) peptides, glutathione-S-transferase (GST), histone deacetylases (HDAC), norepinephrine reuptake (NERI) or cyclooxygenase (COX) inhibitors.[17] While some of these multi-action drugs have shown efficacy *in vitro* and *in vivo*,[18] others had similar activity to the clinically approved Pt(II) drugs.[15-17] It is pertinent to note that the Pt(IV) compounds that entered clinical trials with limited efficacy (like Satraplatin in phase III[12]) did not contain bioactive ligands.[17,18]

Platinum(IV) heterometallic compounds have been described[19] with examples of derivatives containing metals such as ruthenium,[20-23] iron,[24] and lanthanides.[25,26] In general, these compounds have been more active and selective than cisplatin *in vitro* due to synergistic and cooperative effects of the Pt(IV) and second bioactive metal precursors. Two Pt(IV) compounds containing Ru-p-cymene[23] and Gd-texaphyrin[26] fragments resulted very promising *in vivo*. It is surprising that only one article reports on Pt(IV) containing Au fragments so far,[27] despite the impressive antitumor properties displayed by gold compounds. Gold(I) compounds such as antirheumatic FDA-approved Auranofin (Fig. 1**e**) and related compounds have attractive antimigratory, apoptotic, and antiangiogenic properties while causing immunogenic cell death (ICD).[28] Relevantly, a potential synergism of Pt agents and Auranofin in cancer has been hypothesized based on: (1) irreversible toxicity caused by accumulation of reactive oxygen species and irreparable DNA damage; and (2) simultaneous induction of ICD with negative consequences for the survival of the tumor.[29,30] Since 2011 our research group has developed gold-based heterometallic compounds containing iron, titanium or ruthenium, which have shown high efficacy against different cancers (ovarian, prostate and colon).[31,32] Moreover, we reported on highly potent titanium-gold and ruthenium-gold compounds against renal cancer both *in vitro*[31,32] and *in vivo*.[32-36] We have identified three compounds (two Ti-Au: Titanocref and Titanofin,[32-35] and one Ru-Au: RANCE-1[32,36]) as leading candidates for the potential treatment of clear cell renal carcinoma (ccRCC) due to their high efficacy (significant tumor reduction or complete tumor growth inhibition) coupled with no signs of pathological complication.

Recently, the first binuclear Pt(IV)-Au(I) compounds have been reported[27] demonstrating the enormous potential for these type of drugs as anticancer agents. Pt(IV) compounds based on cisplatin, oxaliplatin, and carboplatin containing Au(I)-N-heterocyclic carbene fragments showed high cytotoxicity and selectivity against cancer cell lines and a selected Pt(IV)-Au(I)-NCH compound containing cisplatin an axial phenylbutyrate displayed growth inhibition in Lewis lung carcinoma mouse xenograft models.[27]

We report here on the synthesis, characterization, and stability studies of new heterometallic binuclear PtAu and trinuclear $PtAu_2$ compounds combining bioactive Au(I)-phosphane and Pt(IV) compounds based on cisplatin and oxaliplatin. We describe their anticancer activity and possible biomolecular targets. In contrast to the binuclear Pt(IV)-Au(I) derivatives reported,[27] the compounds described here (Scheme 1) can be obtained directly from platinum(IV) derivatives containing hydroxy groups[37-40] without further modification of axial ligands in the Pt(IV) precursors or the linker attached to gold(I).

Results and Discussion

Synthesis, characterization, and stability of heterometallic compounds

The synthesis of the new Pt(IV)Au(I) compounds is shown in Scheme 1. One equivalent of mononuclear gold(I) compound **Au-2** is reacted with one equivalent of oxo-cisplatin in DMSO at 70 °C for 16 hours yields binuclear PtAu compound $[Pt(NH_3)_2Cl_2(OH)\{(OOC\text{-}4\text{-}C_6H_4\text{-}PPh_2)AuCl\}]$ **PtAu-3** in moderate yield (44%) as an air- and moisture-stable white solid. Compound **Au-2** [Au(Cl)(4-dpb-NHS)] is an activated ester of previously reported Au(I) compound **Au-1** containing chloro and 4-diphenylphosphino benzoic acid (4-dpb) [AuCl(P(Ph_2)-4-C_6H_4-COOH)]. The reaction of compound **Au-1** with coupling reagent tetrafluoroborate benzotriazole tetramethyl uranium (TBTU), triethylamine and the Pt(IV) compounds oxoplatin (hereafter named oxo-cisplatin for clarity) $[Pt(NH_3)_2Cl_2(OH)_2]$ and oxo-oxaliplatin $[Pt(DACH)(C_2O_4)(OH)_2]$ (DACH: diaminocyclohexane) in DMF at room temperature (48 h) affords trinuclear derivatives $PtAu_2$ $[Pt(NH_3)_2Cl_2\{(OOC\text{-}4\text{-}C_6H_4\text{-}PPh_2)AuCl\}_2]$ **$PtAu_2$-4** and $[Pt)(DACH)(C_2O_4)\{(OOC\text{-}4\text{-}C_6H_4\text{-}PPh_2)AuCl\}_2]$ **$PtAu_2$-5**, respectively (Scheme 1) as air- and moisture-stable pale yellow solids in low yields after purification (32% and 25% respectively).

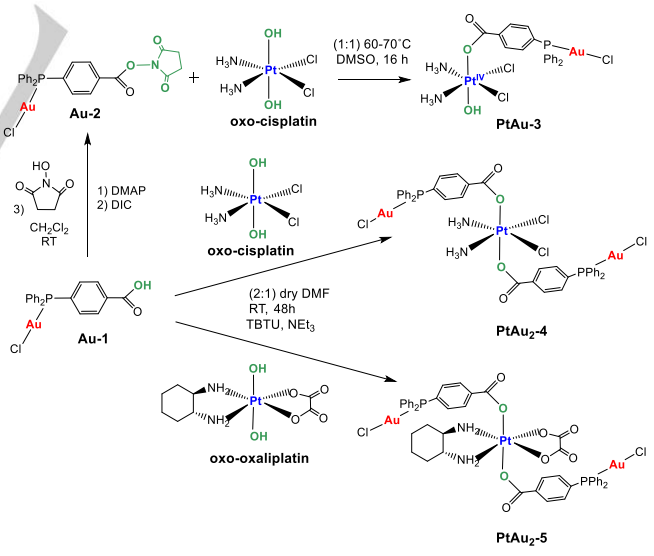

Scheme 1. Preparation of monometallic gold(I) compound **Au-2** and heterometallic binuclear PtAu (**PtAu-3**) and trinuclear $PtAu_2$ compounds (**$PtAu_2$-4** and **$PtAu_2$-5**) via coupling reaction between gold(I) and platinum (IV) precursors.

The structure of these compounds (Scheme 1) are proposed accordant with NMR (Fig. S1-S15), IR spectroscopy (Fig. S17-S20), mass spectrometry (Fig. S21-S22), diffuse reflectance spectroscopy (Fig. S23-S25) and elemental analysis data. Moreover, IR spectroscopy (Fig. S17-S20) and DFT calculations

10.1002/chem.202302045

(Fig. 2) were performed to confirm the coordination mode of the carboxylate groups to the Pt(IV) centers. The solid-state IR spectra of compounds **PtAu-3**, **PtAu$_2$-4** and **PtAu$_2$-5** demonstrate that the carboxylate groups from **Au-1** and **Au-2** starting materials bond to the oxygen from the Pt(IV) hydroxo group as monodentate ligands. The differences between antisymmetric and symmetric stretching bands found are higher than 200 cm^{-1}, 300 cm^{-1} (**PtAu-3**), 311 cm^{-1} (**PtAu$_2$-4**), and 346 cm^{-1} (**PtAu$_2$-5**) (Fig. S17-S20).

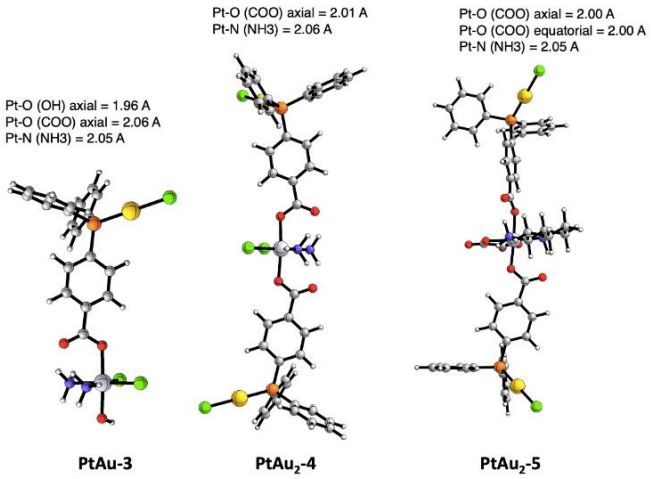

Figure 2. Energy-minimized (DFT) models for heterometallic (**PtAu-3**) and PtAu$_2$ compounds (**PtAu$_2$-4** and **PtAu$_2$-5**). Color code: white, hydrogen; grey, carbon; red, oxygen; blue; nitrogen; orange, phosphorus; green, chlorine; yellow, gold; metallic grey, platinum.

DFT calculations afford theoretical values for these differences supporting the coordination in a monodentate fashion: 277 cm^{-1} (**PtAu-3**), 325 cm^{-1} (**PtAu$_2$-4**), and 316 cm^{-1} **(PtAu$_2$-5**) (Fig. S26-S28).[41-47] The supplementary information section includes optimization data. All optimizations led to compounds containing monodentate carboxylates (Fig. 2). Aiming to further understand the nature of absorption phenomena, the diffuse reflectance spectra of compounds **PtAu-3**, **PtAu$_2$-4** and **PtAu$_2$-5** were experimentally recorded (S23-S25). UV-Vis Spectroscopy could not be used as the signals assigned due to solvents needed to solubilize the compounds (e.g. DMSO) interfered with the expected compounds' signals. Experimental data might be compared with results provided by a time-dependent density functional theory (TD-DFT) approach[41-47] to assess the nature of the excited states involved in the electronic transitions using Gaussian 16 software.[48] Experiments hint demonstrate that the optical profiles consist of a main band at ca. 240 nm (Fig. S23-S25). Theory demonstrate that such signature is associated to a HOMO → LUMO+2 excitation. As illustrated in Fig. S29-S31, the HOMO spread over the Au(I)-phosphane entity while LUMO+2 is more localized on the inner region of the complex as a consequence of the presence of electron-withdrawing groups, e.g., carbonyls and the Pt(IV) metallic center. The electronic promotion observed in the UV-Vis spectra is therefore ascribed to a metal(Au)-to-ligand charge-transfer (MLCT).

The stability in solution of heterometallic compounds **PtAu-3** **PtAu$_2$-4**, and **PtAu$_2$-5** was determined by $^{31}P\{^1H\}$ and ^1H NMR spectroscopy over a 28-day period in DMSO-d$_6$. All heterometallic compounds were very stable in this solvent (>98%, Fig. S32-S38).

Attempts to study the stability in buffer or buffer/DMSO-d$_6$ mixtures were unsuccessful due to poor solubility of the compounds in water-based solutions in the concentration required to measure NMR spectra. Compounds were however soluble at micromolar concentrations in different mixtures such as H_2O/DMSO, PBS/DMSO or media/DMSO (99:1). These mixtures are the usually employed for *in vitro* assays.

Biological activity

Cellular viability, cell death and cellular and organelle uptake

The cytotoxicity of heterometallic PtAu (**PtAu-3**) and PtAu$_2$ compounds (**PtAu$_2$-4** and **PtAu$_2$-5**) was evaluated by Presto Blue assay to quantify cell growth inhibition (Table 1). Human cancer cell lines were used for this assay, which include ovarian carcinomas SKOV-3 and A280, triple negative breast cancer (TNBC) MDA-MB-231, clear cell renal cell carcinoma (ccRCC) Caki-1, bladder carcinoma T24, and lung carcinoma A549. Cells were incubated for 72 hours with the compounds at 37˚C.[49] Non-cancerous human lung fibroblasts (IMR90) were also evaluated. The cytotoxicity and selectivity of heterometallic compounds was compared to that of FDA-approved Pt(II) compounds cisplatin,[50,51] and oxaliplatin,[52] platinum (IV) oxo-cisplatin[53] and oxo-oxaliplatin,[54] and monometallic compound **Au-1**[55,56] (Table 1).

The cytotoxicity of heterometallic compounds in the selected cancerous cell lines is considerably higher in all cell lines (with the exception of ovarian A2780) than that of the Au(I) precursor (**Au-1**) and corresponding Pt(IV) precursors (oxo-cisplatin for **PtAu-3** and **PtAu$_2$-4**) or oxo-oxaliplatin (for **PtAu$_2$-5**). All heterometallic compounds display a cytotoxicity comparable to that of cisplatin and oxaliplatin, with new PtAu compounds being considerably more cytotoxic than oxaliplatin in the ovarian SKOV-3 and bladder T24 cell line. Interestingly, we found that **PtAu$_2$-4** and **PtAu$_2$-5** are more cytotoxic than cisplatin and oxaliplatin for the TNBC MDA-MB-231 cell line, with **PtAu$_2$-5** being 16-fold less toxic with respect to the IMR90 fibroblasts. Similar IC$_{50}$ values have been described for recently reported binuclear PtAu derivatives.[27] Moreover, **PtAu$_2$-5** has a selectivity index larger than 7.7 when comparing the IC$_{50}$ values between lung carcinoma A549 and lung IMR90 fibroblasts (Table 1). We studied the effect of the combination of individual monometallic platinum(IV) oxo-oxaliplatin and gold(I) (**Au-1**) (in 1: 1 and 1:2 mol ratios) in the TNBC MDA-MB-231 cell line (72 h incubation, table S1). We obtained IC$_{50}$ values of 83.7 + 5.1 μM (1:1) and 61.8 + 4.1 μM (2:1) which are considerably higher than the value obtained for **PtAu$_2$-5** in this cell line (5.87 + 0.01 μM). This data supports the hypothesis of improvement of cytotoxic profile by synergism for the Pt-Au complexes in triple negative breast cancer cell lines.
Due to our interest in finding potential chemotherapeutics for TNBC,[49] and the cytotoxicity/selectivity observed, we selected the MDA-MB-231 cell line to further understand the anticancer properties of heterometallic compound **PtAu$_2$-5**. TNBCs are highly metastatic and aggressive, and difficult to be targeted due to the lack of most common receptors usually found in breast cancers.[49]

10.1002/chem.202302045

RESEARCH ARTICLE

Table 1. IC_{50} values (μM) in human cell lines were determined for monometallic compound **Au-1,** monometallic Pt(IV) compounds oxo-cisplatin and oxo-oxaliplatin and heterometallic compounds **PtAu-3, $PtAu_2$-4** and **$PtAu_2$-5** for 72 hours incubation using Presto Blue. Cisplatin and oxaliplatin were used for comparison purposes.[a]

Tissue of Origin	Breast	Ovarian		Renal	Bladder	Lung		Selectivity Index (SI)
Cell line	**MDA-MB-231**	**SKOV-3**	**A2780**	**Caki-1**	**T24**	**A549**	**IMR90**	
cisplatin	7.46 ± 0.62	3.84 ± 0.39	1.40 ± 0.31	3.21 ± 0.88	2.86 ± 0.36	2.22 + 0.03	6.21 ± 0.08	2.7
oxaliplatin	10.14 ± 0.89	42.6 ± 3.6	1.82 ± 0.02	8.21 ± 0.07	>100	15.8 + 0.62	29.8 ± 1.3	1.9
oxo-cisplatin	52.02 ± 0.08	38.6 ± 4.4	2.70 ± 0.40	33.1 ± 2.9	69.9 ± 4.9	67.8 + 2.5	53.5 ± 4.0	0.7
oxo-oxaliplatin	>100	>100	4.03 ± 0.12	>100	>100	>100	>100	N.A[b]
Au-1	16.5 ± 1.0	49.0 ± 5.7	11.53 ± 1.0	45.7 ± 2.6	89.9 ± 7.8	24.9 + 0.62	22.8 ± 5.5	0.9
PtAu-3	7.07 ± 0.51	14.32 ± 2.0	4.58 ± 0.86	5.0 ± 1.2	12.6 ± 1.8	15.0 + 2.1	48.9 ± 5.5	3.2
$PtAu_2$-4	3.20 ± 0.01	7.9 ± 1.4	3.45 ± 0.12	3.21 ± 0.02	7.06 ± 0.48	10.25 + 0.41	30.1 ± 0.89	2.9
$PtAu_2$-5	5.87 ± 0.01	2.99 ± 0.05	9.65 ± 0.90	3.01 ± 0.09	5.42 ± 1.1	12.85 + 0.45	>100	> 7.7

[a] Heterometallic compounds **PtAu-3**, **$PtAu_2$-4**, and **$PtAu_2$-5** and monometallic compound **Au-1** were dissolved in 1% DMSO. Platinum(IV) compounds oxo-cisplatin and oxo-oxaliplatin were dissolved in 0.1% H_2SO_4. Oxaliplatin was dissolved in H_2O. Cisplatin was dissolved in 0.9% NaCl solution. [b] Not applicable: IC_{50} >100 μM.

We then proceeded to evaluate the type of cell death for heterometallic **$PtAu_2$-5**. Platinum(IV) prodrugs and platinum(II) complexes (including cisplatin, oxaliplatin and carboplatin)[7,19] as well as auranofin and several gold(I) compounds,[57,58] are known to induce apoptosis. Cell apoptosis was studied on MDA-MB-231 cells by using Annexin V and propidium iodide (PI) labeling detected of incubation with compound **$PtAu_2$-5**, along with precursors **Au-1**, and Pt(IV) oxo-oxaliplatin by flow cytometry (Fig. S39-S41). FDA-approved Pt(II) oxaliplatin was used for comparison. Data at 24 h is provided in the SI (Fig. S39-S40) which indicated apoptosis of 21.9% for **$PtAu_2$5**. We therefore increased the incubation time to 72 h. At this timepoint, an elevated level of apoptosis is expected for untreated cells.[59] Additionally, commonly used apoptotic inducers such as Staurosporine or Auranofin (IC_{50} concentrations) cannot be used as positive controls at 72h since they kill all cells at IC_{50} concentrations. Figure 3 depicts cell death % (Apoptotic vs Alive) for MDA-MB-231 cells treated with the metal compounds (72 h). **$PtAu_2$-5** showed an increase of early apoptosis of 55% (a similar increase was obtained with the Au precursor **Au-1** at 62%). Heterometallic **$PtAu_2$-5** induces more early apoptosis in the TNBC cell line than oxaliplatin or oxo-oxaliplatin (30% and 22%, respectively). No late-stage apoptosis was generated by any of the monometallic and heterometallic compounds tested after 72 h of incubation (Figure S41). A recent study that included oxaliplatin treatment alone and in combination therapy, demonstrated a 30% increase in apoptosis in MDA-MB-231 TNBC cell line [60] which is comparable to our results, with similar effects seen for cisplatin treated cells.[61] Pt(IV) containing biomolecules in the axial position are not always highly apoptotic,[62] while others have a similar increase of early apoptosis between 30-60%[63,64] comparable to that of **$PtAu_2$-5** heterometallic compound. Carboplatin induced ca. 60% apoptosis in the TNBC MDA-MB-468 cell line.[65] We can therefore state that the apoptotic potency of **$PtAu_2$-5** is comparable or better to that of other FDA approved platinum(II) drugs used in clinic.

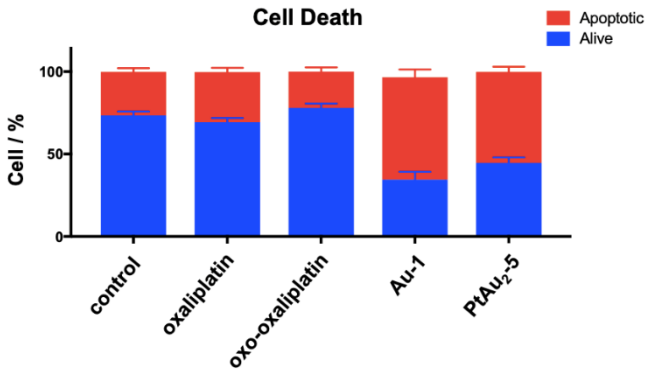

Figure 3. Apoptotic cell death quantitation of oxaliplatin, monometallic starting materials oxo-oxaliplatin and **Au-1**, and heterometallic **$PtAu_2$-5** in MDA-MB-231 cell line using AnnexinV with propidium iodide (PI) labeling analyzed after 72 h of incubation with IC_{50} using flow cytometry. The data reported in the graphs, and standard deviation of the sample mean, from three independent trials.

Next, we analyzed the cellular uptake and colocalization in cytoplasm, nucleus, and mitochondrial compartments for the heterometallic compounds, monometallic **Au-1**, oxo-oxaliplatin, and oxaliplatin. Platinum compounds such as cisplatin, oxaliplatin and carboplatin are known to accumulate in the cell nucleus,[66] while gold compounds typically accumulate in the mitochondria.[67] In order to determine the content of Pt and Au in the cell and cellular organelles, we used Atomic Absorption Spectroscopy (AAS) (Fig. 4). Total Pt and Au accumulation within the whole cell (MDA-MB-231 cell line) for **$PtAu_2$-5** was ~50% for both metals (5.45 ± 0.47 and 4.60 ± 0.37 μg/mL, respectively, Fig. S42). It is remarkable that the stoichiometric ratios of these elements are almost 1:1. This suggests that the compound remains stable in the intracellular environment under incubation conditions as we have observed for other gold(I)-containing heterometallic compounds.[33]

10.1002/chem.202302045
WILEY-VCH

RESEARCH ARTICLE

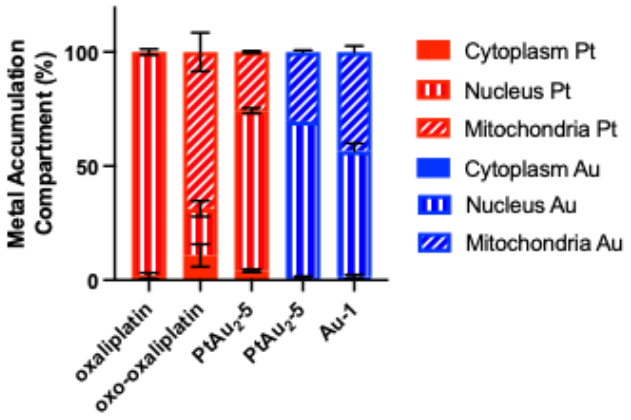

Figure 4. Platinum and gold organelle uptake quantitation of monometallic **Au-1**, oxo-oxaliplatin and oxaliplatin and heterometallic **PtAu₂-5** in MDA-MB-231 cell line using fractionation buffer and centrifugation and analyzed by Atomic Absorption Spectrometry (AAS) after 72 h of incubation with IC_{50}. The data reported in the graphs, and standard deviation of the sample mean, result from three independent trials.

For monometallic control oxaliplatin, Pt content is found to be 98% in the nucleus, as expected.[68] Monometallic Pt(IV) oxo-oxaliplatin accumulates in mitochondria (69%), nucleus (20%) and cytoplasm (11%). Monometallic gold(I) **Au-1** accumulates mainly in nucleus (55%) and in mitochondria (45%). For heterometallic compound **PtAu₂-5**, the content of Pt is found to be 4% cytosol, 70% nucleus and 26% mitochondria whereas the Au content found is 1% cytosol, 69% nucleus and 30% mitochondria (very similar). It seems that **PtAu₂-5** is reaching cellular compartments as a molecule still containing both metal centers, and possibly without having been reduced in the cellular millieu. For a platinum(IV) compound containing biotin,[37] the accumulation of Pt in the nucleus of MDA-MB-231 cells was 16%, suggesting that axial ligand lipophilicity and bulkiness might affect cellular/organelle uptake.[37]

Anticancer activity: inhibition of migration and angiogenesis

The migration of cancer cells is one of the first steps in tumor metastasis.[56] Inhibition of cancer cell migration can be quantified and may serve as indication of anti-metastatic potential of a drug.[56] The antimigratory potential of **PtAu₂-5**. was evaluated by using a wound-healing scratch assay.[69] MDA-MB-231 cell line treatment with **PtAu₂-5** (IC_{20} concentration) slowed down the wound-healing (or inhibited migration) by 95% (Fig. 5 A, B) while precursor **Au-1**, and Pt(II) oxaliplatin (used for comparison) inhibited migration by 40% and 20% respectively (Fig. 5 A, B). The Pt(IV) precursor oxo-oxaliplatin inhibited migration in a similar manner to the vehicle control (0.1% DMSO) around 27%. These results clearly demonstrate impressive anti-migratory properties of **Pt-Au₂-5** which surpass those of other Pt(IV) compounds[62,70] studied in this cell line,[49] and of other Au-based heterometallic compounds with relevant antimigratory properties.

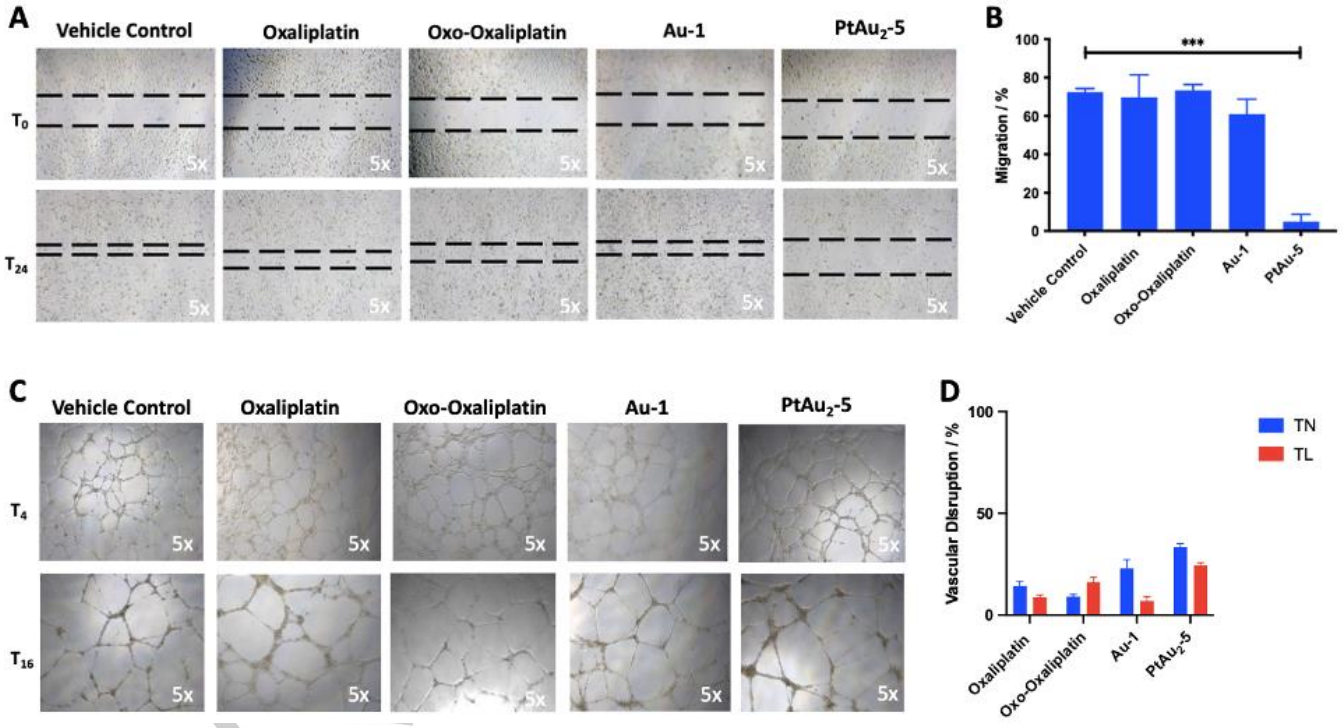

Figure 5. Cell Migration and Endothelial Tube Formation Assays for heterometallic **PtAu₂-5** and monometallic **Au-1**, oxo-oxaliplatin and oxaliplatin compounds. **A)** 2D wound-healing scratch assay showing MDA-MB-231 migration interference images captured at 0 h (top) and 24 h (bottom) post dosing and **B)** migration inhibition quantitation of all compounds after 72 h IC_{20} concentration was added. **C)** Vascular endothelial reorganization images captured at 4h (top) and 16 h (bottom) post dosing and **D)** vascular disruption quantitation in seeded Human Umbilical Vein Endothelial Cells (HUVEC) after 72 h IC_{10} concentration of all compounds was added. The data reported in the graphs, and standard deviation of the sample mean, result from three independent trials averaging quantitation from four fields of view per trial. All images were capture at 5x magnification. 90% confluency was confirmed prior to dosing in each well.

10.1002/chem.202302045

Neovascularization, or endothelial tube formation, is a common trait of cancer cells that is used to gain nutrients necessary for tumor growth.[71] Inhibition of endothelial tube and node formation is an indication of inhibition of angiogenesis and can be quantified. [70] The assay involves the use of human umbilical endothelial cells (HUVEC), which have the ability to form tubular structures when plated on Matrigel, which acts as an extracellular membrane (ECM)-like matrix.[72,73]

HUVEC cells were dosed with heterometallic compound **$PtAu_2$-5**, monometallic **Au-1**, Pt(II) oxaliplatin and Pt(IV) oxo-oxaliplatin at IC_{10} concentrations. HUVEC cells were allowed to vascularize over 16 h to form tubes. The antiangiogenic properties of a compound are correlated to tube formation, defined through the number of lengths (TL) and nodes (TN) as compared to the untreated control, with a lower number associated to higher anti-angiogenic properties (Figure 5 C, D). Compound **$PtAu_2$-5** displays a 34 % disruption of tube nodes and 24.4 % disruption of tube length. For Pt(II) oxaliplatin the disruption is 14% TN and 8% TL. Monometallic starting materials Pt(IV) oxo-oxaliplatin and gold(I) **Au-1** have disruptions of 9% TN and 16% TL, and 23% TN and 7% TL, respectively. It is clear that heterometallic compound **$PtAu_2$-5** displays improved antiangiogenic properties with respect to monometallic Pt(IV) and Au(I) compounds and FDA approved oxaliplatin. Inhibition of cell migration and angiogenesis was not reported for the recently described heterometallic Pt(IV)-Au(I) compounds.[27] A Pt(IV) compound containing the bioactive PDMA ligand specifically designed to inhibit vessel formation, displayed very high anti-angiogenic activity in HUVEC cells.[62]

The combined cytotoxicity, selectivity, apoptotic behavior, anti-angiogenic properties, and extremely relevant anti-migratory properties displayed by **$PtAu_2$-5** in the TNBC MDA-MB-231 cell line, make this compound a promising candidate for further evaluation.

Anticancer activity: 3D TNBC cancer cell model

Conventional 2D cell cultures are not representative models for *in vivo* cancer biology. There is an increasing movement toward the use of *in vitro* 3D culture models as they are more illustrative of the *in vivo* environment. Animal model studies are expensive and more complex to design and analyze.[74] Spheroids, which can be generated for specific cell lines in a reproducible manner, represent a simple methodology that can be used for drug screening in cancer research. They are a more physiologically relevant system than 2D monolayers and resemble more closely the *in vivo* environment by mimicking tissue key factors.[75,76] We generated spheroids of the TNBC MDA-MB-157 carcinoma cell line in a reproducible manner, and set to study the cytotoxicity of selected heterometallic **Pt-Au_2-5.**

We first evaluated the cytotoxicity on MDA-MB-157 cells (PrestoBlue ™ assay, 72 h incubation) for **$PtAu_2$-5**, precursors gold(I) **Au-1**, and platinum(IV) oxo-oxaliplatin. We also used FDA-approved oxaliplatin for comparison (Table 2). Both **$PtAu_2$-5** and **Au-1** diminished the cell viability of MDA-MB-157 at low micromolar concentrations (3-10 µM) with **$PtAu_2$-5** being slightly more cytotoxic than monometallic **Au-1**. In contrast, the precursor Pt(IV) compound oxo-oxaliplatin did not show cytotoxicity in the range of concentrations tested (1-100 µM) while Pt(II) oxaliplatin exhibited moderate cytotoxicity (IC_{50} = 26.6 ± 1.7 µM) in the 2D monolayer cells. The subsequent evaluation of cell viability MDA-MB-157 multicellular spheroids was performed with **$PtAu_2$-5** and **Au-1**. We did not evaluate precursor Pt(IV) oxo-oxaliplatin due to its lack of cytotoxicity at the concentration range used in the 2D cells.

Table 2. IC_{50} values (µM) in 2D and 3D models for MDA-MB-157 cells with compounds **$PtAu_2$-5**, **Au-1**, oxo-oxaliplatin and oxaliplatin after 72 hours incubation with Presto Blue.[a]

	2D	3D
cisplatin	21.6[b]	n.d.
oxaliplatin	26.6 ± 1.7	n.d.
oxo-oxaliplatin	> 100.0	n.d.
Au-1	6.7 ± 1.2	9.4 ± 1.1
$PtAu_2$-5	3.9 ± 0.9	5.2 ± 1.0

[a] Heterometallic compound **$PtAu_2$-5** and monometallic compound **Au-1** were dissolved in 1% DMSO. Platinum(IV) compound oxo-oxaliplatin was dissolved in 0.1% H_2SO_4. Oxaliplatin was dissolved in H_2O. All compounds were diluted with water before addition to cell culture media for 72 h incubation period. [b] Value reported in reference [77]. (n.d. = not determined)

The results (Table 2) showed that the IC_{50} value for **$PtAu_2$-5** is 5.2 ± 1.0 µM while for monometallic **Au-1** is 9.4 ± 1.1 µM spheroids derived from MDA-MB-157 cells. **$PtAu_2$-5** did not show therefore, the frequently decreased drug sensitivity in 3D models when compared to 2D cells, a process called multicellular resistance (MCR), reported for many metal-based compounds.[78] Differences in the sensitivity for cisplatin between 2D and 3D in TNBC models have been reported.[78] IC_{50} values in 3D models for cisplatin were higher than in 2D cells for the 13 TNBC cell lines studied.[78] These results suggest that the anticancer activity of **$PtAu_2$-5**, is not conditioned by redox potential, hypoxic conditions, cell uptake, bioavailability since the compound exert the same behavior in cells monolayer and spheroids.

Interactions with biomolecular targets

Interactions with plasmid and calf thymus DNA in the absence and presence of reducing agents

While platinum(II) species such as oxaliplatin and cisplatin are known to form strong covalent bonds with purine DNA bases,[33, 79-82] octahedral platinum(IV) compounds do not interact directly with nuclear DNA.[53,82] The presence of reducing agents in the intracellular environment of the cell can however activate the platinum(IV) reduction to platinum(II) allowing interactions with DNA to take place.[53,82] While several gold(I) compounds interact with DNA,[83] most do not display these interactions (or interactions are weak or electrostatic in nature). In order to determine the effects of heterometallic PtAu (**PtAu-3**) and $PtAu_2$ compounds (**$PtAu_2$-4** and **$PtAu_2$-5**), monometallic gold(I) derivative **Au-1**, FDA-approved platinum(II) compounds cisplatin and oxaliplatin as well as platinum(IV) precursors on plasmid pBR322 DNA agarose gel (1%), electrophoresis studies were performed (Fig. 6). Two major shapes of the plasmid are expected: OC (open circular or relaxed form, form II) and CCC (covalently closed or supercoiled form, form I). Evidence of metal-DNA binding is supported by changes in the mobility of the drug-

10.1002/chem.202302045

treated lanes. The larger the retardation of a band, the higher the amount of unwind DNA produced (open circular DNA, OC, form II).[33,79-82] Plasmid (pBR322) treatment with increasing concentrations of PtAu (**PtAu-3**) and $PtAu_2$ compounds (**$PtAu_2$-4** and **$PtAu_2$-5**) showed no evidence of OC accumulation at lower or higher metal-DNA molar ratios (Fig. 6). Gels of plasmid treated with platinum(II) species cisplatin and oxaliplatin displayed bands for expected DNA-drug interactions, while those treated with platinum(IV) species oxo-cisplatin and oxo-oxaliplatin did not change using metal-to-DNAbp 0.2, 0.4, 0.6, 0.8 and 1.0 ratios (Fig. 6). It is unusual for platinum(IV) species to interact with DNA without the presence of a reducing agent.[53]

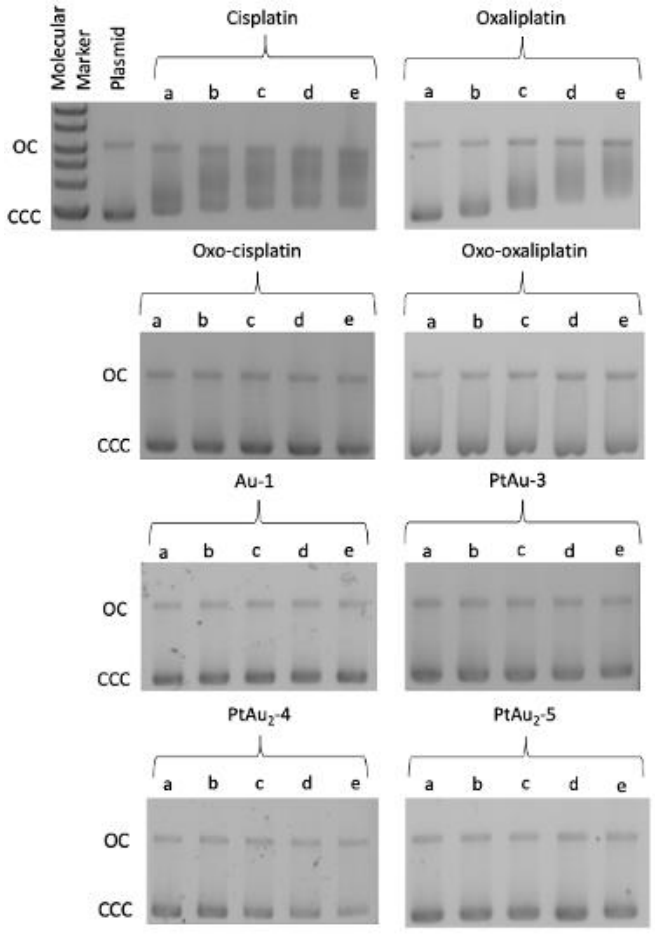

Figure 6. Electrophoresis mobility shift assays for monometallic platinum(II) (cisplatin and oxaliplatin), platinum(IV) (oxo-cisplatin and oxo-oxaliplatin), gold(I) **Au-1**, and heterometallic compounds **PtAu-3**,**$PtAu_2$ -4** and **$PtAu_2$-5**. Plasmid refers to untreated control of DNA plasmid pBR322. (a, b, c, d and e) correspond to metal/DNAbp ratios of 0.2, 0.4, 0.6, 0.8 and 1.0.

Furthermore, DNA-drug interactions can be studied by treating calf thymus DNA (CT-DNA) with drugs and assessing structural changes by Circular Dichroism (CD).[33, 79-82] CT-DNA displays a positive band at 273 nm (base stacking) and a negative band at 242 nm (ellipticity). [33, 79-82] As mentioned before, while platinum(II) (cisplatin and oxaliplatin) are expected to interact with DNA, platinum(IV) (oxo-cisplatin and oxo-oxaliplatin) typically do not (Figure S43). CT-DNA treated with gold compound **Au-1**, bimetallic (**PtAu-3**), and trimetallic compounds (**$PtAu_2$-4**, **$PtAu_2$-5**) using a metal-to-DNAbp ratio of 0.1, 0.25, 0.5 and 1.0 ratio, did not show a significant shift decrease in the base stacking or significant ellipticity perturbations (Fig. S44). These results are indicative of lack of DNA-drug interactions. It is important to note that **Au-1** and heterometallic compounds have low water and buffer solubility. CD spectroscopy experiments were limited to lower concentrations since higher concentrations interfered with the instrument signal.

Gel electrophoresis was performed to study the effects of heterometallic binuclear (**PtAu-3**) and trinuclear compounds (**$PtAu_2$-4** and **$PtAu_2$-5**), monometallic gold(I) derivative **Au-1** and platinum(IV) precursors oxo-cisplatin and oxo-oxaliplatin on plasmid (pBR322) DNA upon reduction with ascorbic acid (AsA) and glutathione (GSH)[82] (Fig. S45-S46). Ascorbic acid is a two-electron reducing agent present in the cytosol at a concentration of ~1mM and known to successfully reduce platinum(IV) to platinum(II). GSH is a cysteine thiol residue and a one-electron reducing agent which is also present in the cytosol microenvironment at concentrations of ~2 mM.[82] For the purpose of the experiments, AsA and GSH were used in a one-to-one equivalent ratio, or one-to-two equivalent ratio, with respect to monometallic or heterometallic compounds.[82] Metal-DNA binding is evidenced by changes in band mobility.

Plasmid pBR322 treatment with 1:1 equivalent of **PtAu-3** -to-AsA provided evidence of a delay in the band mobility indicative of DNA-drug interaction, while treatment with **PtAu-4** or **PtAu-5** did not. Furthermore, gels of plasmid (pBR322) DNA treated with heterometallic compounds did not display changes in band mobility upon GSH addition (1:2 equivalent of metal complex-to-GSH). We also studied the interactions of CT-DNA with the metal-based compounds by CD spectroscopy[33,79-82] upon the treatment with reducing agents[82] AsA and GSH utilizing the same equivalent of metal-to-DNAbp ratio. Spectra of CT-DNA treated with heterometallic compounds and ASA (1:1 ratio) showed slight modifications but no significant alteration of the CT-DNA base stacking and ellipticity conformation (Fig. S47). Experiments using reducing agent GSH in a one-to-two ratio were inconclusive due to interactions between the reducing agent GSH and the CT-DNA (data not provided).

To summarize, experiments of plasmid- or CT-DNA treated with Pt(IV)-Au(I) heterometallic compounds without a reducing agent, did not show binding or changes to the structural conformation of the DNA. Compound **PtAu-3** showed interactions with plasmid- or CT-DNA upon treatment with 1:1 equivalent of AsA reducing agent while compounds **$PtAu_2$-4** and **$PtAu_2$-5** did not. DFT calculations support that the reduction occurs more favorably in the order **PtAu-3** > **$PtAu_2$-4** > **$PtAu_2$-5** (Fig. S48). We can infer that the type of axial ligand influences the Pt(IV)→Pt(II) reduction facilitating it in the case of mono-substituted **PtAu-3** Several Pt(IV) monometallic compounds have shown to be reduced *in situ* and interact with CT DNA[37,62,84] but Pt(IV) octahedral structures can be very stable depending on the coordinated ligands. In fact, this stability can play a role of reduction inertness or very slow reduction.[85] Specifically, the composition of the equatorial ligands can dictate the kinetic inertness of a Pt(IV) compound.[85] For example, compounds containing bidentate oxalato equatorial ligands may be more stable than those containing equatorial dichlorido ligands.[85] It is known that Pt(IV) compounds incorporating the oxaliplatin core, and coordinated directly to carboxylate-containing axial ligands, do not reduce easily to platinum(II).[24,86] In order to optimize second generation

Pt(IV)-Au(I) compounds, we should modify the chemical structure by adding a carbonate or carbamate bridge between the Pt(IV) and the axial ligand to favor reductive activation conditions. This structural change can significantly increase the ability of the Pt core to produce DNA damage upon fast reduction inside the cellular space.[18] The reduction of binuclear Pt(IV)-Au(I)-NHC compounds containing an axial ligand coordinated through a carbamate group[27] was demonstrated by HPLC and MS. Reduced Pt(II) fragments could be identified in some cases upon treatment, using a very high concentration of AsA (10 equivalents).[27] Interactions with telomeric DNA (G-quadruplex, G4)[83] will need to be explored in the near future, to exclude this biomolecule as potential target. This is relevant since organelle uptake in MDA-MB-231 cells indicates high Pt and Au accumulation for trinuclear compound **PtAu$_2$-5** in the cell nucleus.

Thioredoxin reductase (TrxR) inhibition

Thioredoxin reductase (TxrR) is an enzyme playing a vital role to preserve the redox balance in cells which leads to critical cellular functions such as cell growth, apoptosis, and DNA synthesis. To gain a mechanistic insight, we investigated if heterometallic compounds inhibited TxrR in MDA-MB-231 cells. Compounds were first tested at IC_{50} concentrations (72-hour incubation) and quantified through a colorimetric assay. Gold compounds are typically known to inhibit TrxR[67,87] while platinum compounds are more likely to critically target DNA integrity.[33,79-82] Monometallic compounds Pt(IV) (oxo-cisplatin and oxo-oxaliplatin) and Au(I) (**Au-1**) were also tested to help with data deconvolution. Cisplatin, oxaliplatin and auranofin were used as controls.

As expected, inhibition of TrxR activity (%) at IC_{50} concentrations was lowest for oxaliplatin (29.7%) and cisplatin (26.4%), and highest for Auranofin (100%) [67,87] (Fig. 7A). Inhibition of enzyme activity for **Au-1** and platinum(IV) oxo-cisplatin was similar 67.1% and 66.0%, respectively, (Fig. 7A) while platinum(IV) oxo-oxaliplatin at IC_{50} concentration (>100 μM) afforded 100% inhibition (Fig. 7A). Heterometallic compounds **PtAu-3**, **PtAu$_2$-4** and **PtAu$_2$-5** also demonstrated near complete or complete inhibition (97.4-100%) like Auranofin at IC_{50} concentrations (Fig. 7A). We performed an experiment with lower concentrations (1 μM) for the compounds which had afforded higher TrxR inhibition (auranofin, **PtAu$_2$-5**, and oxo-oxaliplatin). Enzyme activity inhibition (1 μM of metal compound) was 13.5% for oxo-oxaliplatin, 47.3% for **PtAu$_2$-5** and 100% for Auranofin (Fig. 7B). We can conclude that **PtAu$_2$-5** acts as a good inhibitor of TrxR activity, and that the Pt(IV) core has a strong influence as it inhibits TrxR better than gold(I) fragment **Au-1**. Previously reported heterometallic compounds containing Ti(IV) and the same Au(I) moiety resulted in TrxR inhibition in renal Caki-1 cells.[33] A binuclear Pt(IV)-Au(I) compound containing an Au(I)-NHC fragment and phenylbutyrate as axial ligand, displayed TrxR inhibition in lung cancer cell line (A549) after 24 h incubation (5.5 μM, 22-fold higher than the IC_{50} in this cell line).[27] The inhibition of TrxR *in vivo* was also demonstrated. In general, all Pt(IV)-Au(I) reported displayed inhibition of the isolated enzyme at nanomolar concentrations, but the involvement of direct binding of Au(I) to selenocysteine did not seem to be the only factor for this inhibition.[27]

Our results in the highly proliferative and aggressive TNBC MDA-MB-231 cell line, indicate that the trinuclear derivative **PtAu$_2$-5** inhibits TrXR efficiently at concentrations 1/5 of the IC_{50} value in this cell line.

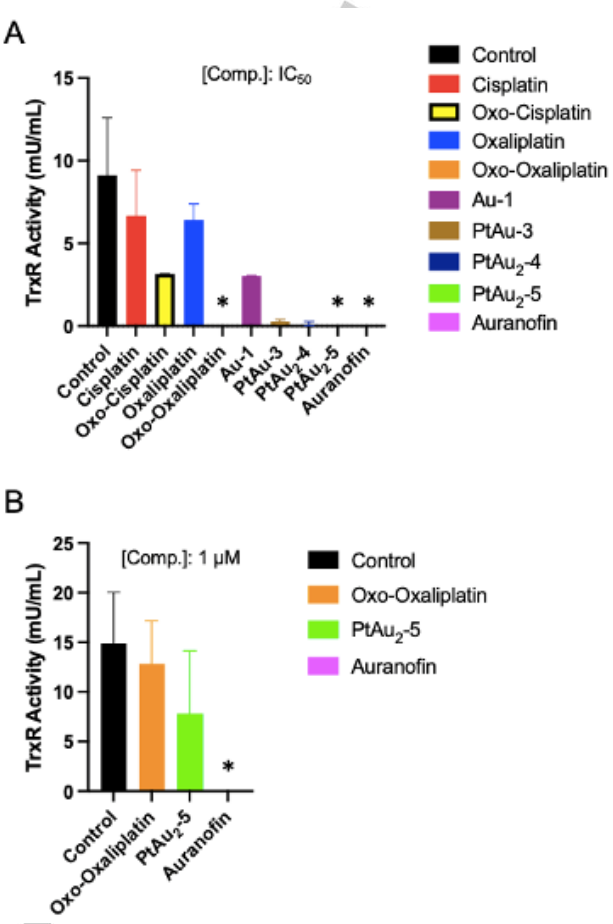

Figure 7. Inhibition of pro-angiogenic protein in MDA-MB-231 TNBC cells. **A)** Inhibition of mitochondrial protein TrxR at IC_{50} concentration by monometallic Au(I), Pt(II) and Pt(IV) compounds and heterometallic compounds **PtAu-3**, **PtAu$_2$-4**, and **PtAu$_2$-5**, and auranofin at 72 h. **B)** Inhibition of TrxR enzyme by oxo-oxaliplatin, **PtAu$_2$-5** and auranofin (1μM) at 72 h. The values indicate concentration per milliliter of TrxR activity inhibition relative to the control (DMSO 0.1%). (*= enzyme activity completely inhibited at the concentration tested).

Conclusion

We have developed binuclear PtAu and trinuclear $PtAu_2$ Pt(IV)-Au(I) compounds based on cisplatin and oxaliplatin cores and gold-chloro fragments coordinated to a phosphane-carboxylate linker able to directly bind to hydroxo axial ligands of the Pt(IV) precursors. The compounds are highly potent *in vitro* against a panel of breast, ovarian, renal, bladder, and lung cancerous cell lines.

We selected trinuclear compound **PtAu$_2$-5**, containing the oxaliplatin core, for further studies due to its cytotoxicity and high selectivity profile against TNBC cells. This compound exerts apoptosis and accumulates in the nucleus and mitochondria. Through a series of biological assays comparing the efficacy of **PtAu$_2$-5** with oxaliplatin, monometallic platinum(IV) oxo-oxaliplatin and gold(I) precursor (**Au-1**), we demonstrated the extremely high effectivity of **PtAu$_2$-5** inhibiting cell migration in MDA-MB-231 cells and its high antiangiogenic properties.

Moreover, **PtAu$_2$-5** has a potent cytotoxicity against TNBC 3D spheroids. While trinuclear compounds do not seem to display relevant interactions with plasmid (pBR322) and CT DNA even in the presence of reducing agents such as ascorbic acid or glutathione, binuclear **PtAu-3** displayed DNA-drug interactions upon treatment with one-to-one equivalent of AsA reducing agent for treated plasmid and CT-DNA. The hydroxo axial ligand present in **PtAu-3**, instead of a second Au-containing molecule, may facilitate the reduction of the Pt(IV) and further interaction with DNA. We have also demonstrated that **PtAu$_2$-5** inhibits TrxR in TNBC cells at concentrations as low as a fifth of the IC_{50} value in these cells.

Our results highlight the potential of these heterometallic compounds as TNBC agents, and warrant further preclinical studies with selected/optimized compounds. In addition, this research expands on the improved pharmacological properties of multimetallic and other anticancer agents by inclusion of bioactive gold(I) components.

Experimental Section

Synthesis and Characterization

All common laboratory chemicals were purchased from commercial sources and used without further purification (Sigma-Aldrich, AmBeed and Strem Chemicals). Cisplatin[7], oxaliplatin[7], oxo-cisplatin,[40] oxo-oxaliplatin[40] and **Au-1**[52] were prepared as previously reported.

NMR spectra were obtained in a BRUKER AV400 ^{1}H NMR at 400 MHz, $^{13}C\{^1H\}$ NMR at 100.6 MHz, $^{31}P\{^1H\}$ NMR at 161.9 MHz and ^{195}Pt NMR at 86.02 MHz. The chemical shifts (δ) were collected using deuterated solvents $CDCl_3$, DMSO-d_6 and D_2O, unless otherwise stated. For ^{1}H NMR and $^{13}C\{^1H\}$ NMR, chemical shifts were referenced to tetramethylsilane (TMS = 0 ppm). Chemical shifts for $^{31}P\{^1H\}$ NMR were referenced to H_3PO_4 (85%) and chemical shifts for ^{195}Pt NMR peaks were referenced to K_2PtCl_6 = 6.6 ppm. The coupling constants (*J-value*) are given in hertz (Hz). IR spectra (4,000-250 cm^{-1}) was recorded in a Nicolet 6700 Fourier transform infrared spectrophotometer on solid-state using the Attenuated Total Reflectance (ATR) accessory. Mass spectra electrospray ionization high resolution (MS-ESI-HR) were performed by direct injection on an Agilent 6550 iFunnel QToF. Elemental analyses were performed on a Perkin-Elmer 2400 CHNS/O series II analyzer by Atlantic Microlab Inc. (US). The theoretical isotopic distributions have been calculated using Molecular Weight Calculator v6.50.

[Au(Cl)(4-dpb-NHS)] (Au-2). In a schlenk flask, [AuCl(4dpb)] **Au-1** (500 mg, 1 eqv) was solubilized in dichloromethane (10 mL). Subsequently, DMAP (56 mg, 0.5 eqv) and DIC (117 mg, 1 eqv) were added to the reaction mixture. After 30 minutes, N-hydroxysuccinimide (160mg, 1.5 eqv) was added to the mixture. After 4 hours, the reaction mixture was concentrated to dryness. The yellow solid was collected by filtration and washed with heavy amounts of water (20 mL x10) to remove the urea side product. The solid was washed with diethyl ether (5 mL x3) and left drying overnight. The collected white solid yield was 61%. Anal. Calcd for $C_{23}H_{18}AuClNO_4P$ (635.78): C, 43.45; H, 2.85; N, 2.20. Found: C, 43.66; H, 3.01; N, 2.10. $^{31}P\{^1H\}$ NMR ($CDCl_3$): δ 33.25. $^{31}P\{^1H\}$ NMR (DMSO-d_6): δ 32.93. ^{1}H NMR (DMSO-d_6): δ 8.29-8.26 (2H, *d*, $CH_{2(arom)}$), δ 7.81-7.76 (2H, *dd*, $CH_{2(arom)}$), δ 7.71-7.59 (12H, *m*, $Ph_{2(arom)}$) δ 2.91 (4H, *s*, CH2-$CH_{2(ammine)}$. $^{13}C\{^1H\}$ NMR (DMSO-d_6): δ 170.64 (s, $C{=}O_{(NHS)}$), δ 157.24 (s, $C{=}O_{(carboxylate)}$), 135.11 (d, $^1J_{PC}$ = *13 Hz,* 3,3'-C_6H_4), δ 134.98 (d, $^1J_{PC}$ = *13 Hz,* 3,3'-C_6H_4), δ 134.68-134.54 (d, $^2J_{PC}$ = *14 Hz,* 2,2'-C_6H_5), δ 134.54 (d, $^2J_{PC}$ = *14 Hz*, 2,2'-C_6H_5), δ 133.20 (d, $^3J_{PC}$ = *3 Hz,* 4-C_6H_4), 131.24 (d, $^4J_{PC}$ = *12 Hz,* 3,3'-C_6H_5), 131.12 (d, $^4J_{PC}$ = *12 Hz,* 3,3'-C_6H_5), δ 130.40 (d, $^5J_{PC}$ = *12 Hz,* 2,2'-C_6H_4), δ 130.28 (d, $^5J_{PC}$ = *12 Hz,* 2,2'-C_6H_4), δ 127.92 (s,1-C_6H_5), δ 127.35 (s, s,4-C_6H_5).

[Pt(NH$_3$)$_2$Cl$_2$(OH){(OOC-4-C$_6$H$_4$-PPh$_2$)AuCl}] (PtAu-3). In a round bottom flask, oxo-cisplatin (0.1 mmol, 33.4 mg) was added to anhydrous dimethylsulfoxide [DMSO, $(CH_3)_2SO$, 5 mL)] and the mixture heated at 70˚C. **Au-2** (0.1 mmol, 63.5 mg) was subsequently added to the suspension. After 16 hours, the reaction mixture was filtered through celite to remove any unreacted platinum or side products. The yellow filtrate was treated with water to precipitate the white solid and collected by filtration. The solid was cleaned with CH_2Cl_2, water and Et_2O (x3 each). The yield of the solid was 44%. Anal. Calcd for $C_{19}H_{21}AuCl_3N_2O_3PPt$ (854.76): C, 26.70; H, 2.48; N, 3.28. Found: C, 26.71; H, 2.65; N, 3.06. ^{195}Pt NMR (DMSO-d_6): δ 1035. $^{31}P\{^1H\}$ NMR (DMSO-d_6): δ 32.25. ^{1}H NMR (DMSO-d_6): δ 8.04-8.02 (2H, *m*, $CH_{2(arom)}$), δ 7.66-7.54 (12H, *m*, PPh_2 + $CH_{2(arom)}$), δ 6.18-5.93 (6H, *t*, $^1J_{HH}$ = *56 Hz,* $2NH_3$). $^{13}C\{^1H\}$ NMR (DMSO-d_6): δ 172.65 (s, C=O), δ 138.73 (s, 3-C_6H_4), δ 134.39 (d, $^1J_{PC}$ = *13 Hz,* 4-C_6H_4), δ 134.01(d, $^2J_{PC}$ = *14 Hz,* 2-C_6H_5), δ 132.91 (d, 3-C_6H_5), δ 130.63 (d, $^3J_{PC}$ = *12 Hz*, 1-C_6H_4), δ 130.26 (d, $^4J_{PC}$ = *12 Hz,* 2-C_6H_4), δ 128.82 (s, 1-C_6H_5), δ 128.20 (s, 4-C_6H_5). IR (cm^{-1}): 3183 w (NH_2), 3055 w (OH), 1635 s (ν_{asym} CO_2), 1333 vs (ν_{sym} CO_2), 1098 vs (ν Pt-O)**.**

[Pt(NH$_3$)$_2$Cl$_2${(OOC-4-C$_6$H$_4$-PPh$_2$)AuCl}$_2$] (PtAu$_2$-4). Au-1 (268 mg, 0.5 mol, 2.5 equiv), triethylamine (83 uL, 1.2 equiv), and TBTU (191 mg, 1.2 equiv) were stirred in dry DMF (5 mL). After 30 minutes, oxo-cisplatin (66 mg, 0.2 mmol) was added. 48 hours later, the reaction mixture was filtered through celite to remove any unreacted platinum or side products. The yellow filtrate was treated with water to precipitate a yellow-white solid from the solution. Later, the solid was collected by filtration and treated with water and diethyl ether (5 mL x3 each). The solid was then solubilized in dichloromethane (10 mL) and extracted with Brine solution (15 mL x5). The organic phase was recovered dried with magnesium sulfate. Then, the heterogenous solution was filtrated by gravity to collect the organic phase. The organic phase was treated with diethyl ether (10 mL) to precipitate a pale-yellow solid for a seond time. The yield was 32%. Anal. Calcd for $C_{38}H_{34}Au_2Cl_4N_2O_4P_2Pt{\bullet}0.65C_3H_7NO{\bullet}0.90C_4H_{10}O$ (1375.48): C, 35.54; H, 2.77; N, 2.90. Found: C, 35.11; H, 3.22; N, 2.49. ^{195}Pt NMR (DMSO-d_6): δ 1192. $^{31}P\{^1H\}$ NMR (DMSO-d_6): δ 32.35. ^{1}H NMR (DMSO-d_6): δ 8.07-8.05 (4H, *m*, $CH_{2(arom)}$), δ 7.62-7.59 (24H, *m*, PPh_2 + $CH_{2(arom)}$), δ 6.75 (6H, *t*, $2NH_3$). $^{13}C\{^1H\}$ NMR (DMSO-d_6): δ 172.50 (s, C=O), δ 136.71 (s, 3,3'-C_6H_4), δ 134.43 (d, $^1J_{PC}$ = *13 Hz,* 4,4'-C_6H_4), δ 134.12 (d, $^2J_{PC}$ = *14 Hz,* 2,2'-C_6H_5), δ 132.94 (d, 3,3'-C_6H_5), δ 130.68 (d, $^3J_{PC}$ = *12 Hz*, 1,1'-C_6H_4), δ 130.28 (d, $^4J_{PC}$ = *11 Hz,* 2,2'-C_6H_4), δ 128.70 (s, 1,1'-C_6H_5), δ 128.09 (s, 4,4'-C_6H_5). IR (cm^{-1}): 1627 s (ν_{asym} CO_2), 1316 vs (ν_{sym} CO_2), 1104 vs (ν Pt-O)**.**

[Pt(DACH)(C$_2$O$_4$){(OOC-4-C$_6$H$_4$-PPh$_2$)AuCl}$_2$] (PtAu$_2$-5). Au-1 (269 mg, 0.5 mol, 2.5 equiv), triethylamine (83 uL, 1.2 equiv), and TBTU (192 mg, 1.2 equiv) were stirred in dry DMF (5 mL) After 30 minutes, oxo-oxaliplatin (86 mg, 0.2 mmol) was then added. 48

hours later, the yellow solution collected was treated with water to precipitate a dark yellow solid precipitated from the solution. The dark yellow solid was collected by filtration and treated with water and diethyl ether (5 mL x3 each). The solid was then solubilized in dichloromethane (10 mL) and extracted with Brine solution (15 mL x5). The organic phase was recovered dried with magnesium sulfate. Then, the heterogenous solution was filtrated by gravity to collect the organic phase. The organic phase was treated with diethyl ether (10 mL) to precipitate solid for a second time. The yield was 25%. Anal. Calcd for $C_{46}H_{42}Au_2Cl_2N_2O_8P_2Pt \bullet 0.50C_6H_{14}$ (1472.72): C, 38.83; H, 3.26; N, 1.85. Found: C, 39.18; H, 3.03; N, 2.30.^{195}Pt NMR (DMSO-d_6): δ 1620. $^{31}P\{^1H\}$ NMR (DMSO-d_6): δ 32.48. ^{1}H NMR (DMSO-d_6): δ 8.12-8.06 (4H, *m*, $CH_{2(arom)}$), δ 7.67-7.54 (24H, *m*, PPh_2 + $CH_{2(arom)}$), δ 2.77 (2H, *s*, $CH_{2(cyclo)}$), δ 2.13 (2H, *s*, $CH_{2(cyclo)}$), δ 1.51-1.49 (4H, *s*, $CH_{2(cyclo)}$), δ 1.23-1.21 (2H, *s*, $CH_{2(cyclo)}$). $^{13}C\{^1H\}$ NMR (DMSO-d_6): δ 171.55 (s, C=O), δ 134.47 (s, 3,3'-C_6H_4), δ 134.34 (d, $^1J_{PC}$ = *13 Hz,* 4,4'-C_6H_4), 134.20 (d, $^1J_{PC}$ = *5 Hz,* 4,4'-C_6H_4), δ 134.15 (d, $^2J_{PC}$ = *5 Hz,* 2,2'-C_6H_5), δ 132.94 (s, 3,3'-C_6H_5), δ 130.76 (d, $^3J_{PC}$ = *22 Hz*, 1,1'-C_6H_4), δ 130.54 (d, $^4J_{PC}$ = *12 Hz,* 2,2'-C_6H_4), δ 130.42 (d, $^4J_{PC}$ = *12 Hz,* 2,2'-C_6H_4), δ 130.28 (d, $^5J_{PC}$ = *12 Hz,* 2,2'-C_6H_4), 130.16 (d, $^5J_{PC}$ = *12 Hz,* 2,2'-C_6H_4), δ 128.60 (s, 1,1'-C_6H_5), δ 127.99 (s, 4,4'-C_6H_5), δ 61.60 (1,1'-$C_6H_{10(cyclo)}$), δ 31.24 (2,2'-$C_6H_{10(cyclo)}$), δ 24.09 (3,3'-$C_6H_{10(cyclo)}$) . IR (cm^{-1}): 2920 s (N-H), 2850 s (N-H), 1637 s (ν_{asym} CO_2), 1291 vs (ν_{sym} CO_2), 1098 vs (ν Pt-O)**.**

Computational Calculations

The geometry of the heterometallic compounds **PtAu-3, $PtAu_2$-4** and **$PtAu_2$-5** were fully optimized within the density functional theory (DFT) framework by using ωB97X-D, a long-range corrected hybrid density functional that includes dispersion. This approach provides confident outcomes for the evaluated structures and optical properties specifically for platinum derived compounds. To describe all the atoms the def2-SVP basis set was used (except the Pt centers). To account for scalar relativistic effects without increasing the computational cost the core electrons were replaced by the effective core potentials def2-ECP. Ultrafine grid for numerical DFT integration was used for all calculations. Vibrational analysis confirms the stable nature of the located minima and lead to the simulated IR spectra. Time dependent DFT (TD-DFT) calculations were performed to predict main optical signatures. To address solvation impact into metallodrugs properties, environmental effects were included by using the polarizable continuum method of Tomasi and co-workers. Gaussian16 was used for all optimizations.

Cell Culture

Human clear cell renal cell carcinoma (ccRCC) line Caki-1, human urinary bladder carcinoma line T-24, human ovarian adenocarcinoma line SKOV-3 and A2780, human breast adenocarcinoma MDA-MB-231, human lung carcinoma A549 and human lung fibroblast line IMR90 were obtained from the American Type Culture Collection (ATCC; Manassas, Virginia, USA) and cultured with appropriate media type including: Dulbecco's modified Eagle's medium (DMEM; Fisher Scientific), Rosewell Park Memorial Institute medium (RPMI), McCoy's5A medium or Ham's F-12K (Kaign's) medium. All media types contained 10 % fetal bovine serum (FBS; Fisher Scientific), 1 % minimum essential media (MEM) nonessential amino acids (NEAA; Fisher Scientific), and 1 % penicillin–streptomycin (PenStrep; Fisher Scientific). Cells were cultured at 37 °C under 5 % CO_2 and 95 % air in a humidified incubator.

Cell Viability Assay

The determination of cytotoxic profiles (IC_{50}) of relevant compounds employed the use of human Caki-1, T-24, SKOV-3, A2780, MDA-MB-231, A549 and IMR90 cell lines for a cell viability assay. Cells were seeded at a concentration of 5.6×10^3 – 6×10^3 cells per well in 100 μL of appropriate complete media into 96-well flat-bottom plates and grown at 37 °C under 95 % air and 5 % CO_2 for 24 h in a humidified incubator. Monometallic gold and heterometallic compounds PtAu and $PtAu_2$ were dissolved in DMSO, oxo-cisplatin and oxo-oxaliplatin were dissolved in a 0.1% H_2SO_4 solution and oxaliplatin and cisplatin were dissolved in 0.9% NaCl solution. Dilutions ranging from 0.5-100 μM for all compounds and controls were added, directly followed by a 72 h incubation period. To quantitative measure the viability of treated cells, PrestoBlue was used. PrestoBlue was added to the cells at a final concentration of 1x and incubated for 1 h at 37 °C under 5 % CO_2 and 95 % air in a humidified incubator. The optical fluorescence was measured at 560/590 nm on a BioTek Synergy Multi-mode microplate reader (BioTek Instruments, Inc., Winooski, VT, USA). The percentage of surviving cells was calculated from the ratio of absorbance of treated to untreated cells. Data is presented as mean ± SEM of at least three independent experiments, each with triplicate measurements.

Cell Death Assay

For the assessment of cell death, cells were cultured in 100-mm tissue culture dishes with appropriate media type and allowed to reach ≈80 % confluency. An IC_{50} concentration of each compound was incubated for 72 h at 37 °C under 95 % air and 5 % CO_2 in a humidified incubator. Following cellular collection through trypsinization, $1x10^6$ cells per sample was prepared using a hemocytometer to count cells. the eBioscience Annexin V-FITC Apop Kit (Invitrogen, Carlsbad, CA) was used according to instructions provided to label cells with 5 μL propidium iodide and 5 μL Annexin V dye. Following a 15 min incubation at room temperature, the dye's fluorescence intensity was detected via flow cytometry with the use of a BD C6 Accuri flow cytometer. 10×10^5 events per sample were recorded. The flow cytometer was calibrated prior to each use.

Cellular and Organelle Uptake

Whole cell and cellular compartment samples were prepared for atomic absorption spectrometry by digestion with 10X volume of concentrated nitric acid and incubation at 85°C for 2 hours. This was followed by the samples being evaporated at 120°C for 2-3 hours. Dried samples were reconstituted in a 10% hydrochloric acid/5% nitric acid solution. Prepared samples were then analyzed for metal content on the AAnalyst 400 (Perkin Elmer) on a wavelength of 242.8 nm for Au and 265.9 for Pt.

Cell Migration Assay

MDA-MB-231 cells were seeded onto a six-well plate coated with fibronectin and grown to a monolayer of ≈ 90 % confluency. Following monolayer formation, a scratch was induced using a p-200 (200 μL) pipet tip. Serum-free media was used following aspiration of complete medium and cells detached due to the scratch. The anti-migratory properties of compound **$PtAu_2$5**, monometallic gold **Au-1**, oxaliplatin and oxo-oxaliplatin were

assessed by treatment with IC_{20} concentrations of each compound. Cells were incubated at 37 °C under 5 % CO_2 and 95 % air in a humidified incubator over 24 h. At 0 and 24 h post-scratch, cells were photographed using a Leica MC120 HD mounted on a Leica DMi1 microscope at 5x magnification.

Endothelial Tube Formation Assay

Anti-angiogenic properties were assessed with the use of human umbilical vein endothelial cells (HUVECs). Geltrex®, Reduced Growth Factor Basement Membrane Matrix (Invitrogen) was used to coat each well of a 96-well plate and incubated at 37 °C for 1h to allow gelation to occur. A density of $25x10^3$ cells/well of HUVECs were added onto the gel layer the presence of monometallic and heterometallic compounds using its IC_{10} concentration. The diluting agent of 0.1% DMSO (as applied to **$PtAu_2$-5** and **Au-1**) served as a control Cells were incubated under 37 °C and 5% CO_2 and then observed at both 4h and 16h time points using Leica MC120 HD mounted on a Leica DMi1 microscope at 5x magnification.

Multicellular Spheroids Development (3D Cell Viability)

MDA-MB-157 cells were seeded for 24h in a 96-multiwell dish, and treated with different concentrations (0.5 to 100 μM) of **Au-1**, **$PtAu_2$-5**, oxaliplatin and oxo-oxaliplatin at 37 °C for 72 h. Next, the medium was changed, and cells were incubated with 0.2 mg/ml of the PrestoBlue ™ for 1 h. Multicellular tumor spheroids were formed with MDA-MB-157 cells using the liquid overlay method. Spheroids were generated by seeding single cell suspension (10×10^3 cells/well) in agarose-coated 96-well plates and cultured in complete medium (with 2% of Matrigel) under standard conditions for 72 h. Multicellular spheroids derived from MDA-MB-157 cells were treated in 96-well plates with 0.5% DMSO in DMEM (control), with **$PtAu_2$-5** (0.5 to 25 μM) and **Au-1** (0.5 to 25 μM) in a range of concentration for 24 h. Cell viability of spheroids was subsequently evaluated by the PrestoBlue ™.

Electrophoresis Mobility Assay

p*B*R322 plasmid DNA (2 μL, 20 μg/mL final concentration) in buffer (5 mM Tris/HCl, 50 mM $NaClO_4$, pH = 7.39) was used for electrophoresis studies. 10 μL total sample volume was incubated with different concentrations of heterometallic compounds **PtAu-3, $PtAu_2$-4** and **$PtAu_2$-5** (0.20, 0.4, 0.6,0.8 and 1.0 metal complex:DNAbp) at 37 ºC in the dark for 20 h. Following the incubation period, a 1% agarose gel was used to load samples. The samples separated by electrophoresis at 100V for 1 h in 1X Tris-acetate/EDTA buffer (TAE). GelRed Nucleic Acid (45 μL in 100 mL of 1X TAE buffer) was used to stain the gel for 30 min immediately after. The gel was visualized using a LI-COR instrument at 600 nm wavelength. For the studies under reductive conditions using ascorbic acid (AsA) was used in a one-to-one equivalent (0.50-to-0.50) and glutathione (GSH) in a one-to-two equivalent (0.50-to-1.0) metal-to-reducing agent ratio while maintaining a 0.50-to-1.0 metal-to-DNA ratio in a total volume of 10 μL.

Circular Dichroism

Freshly prepared calf thymus (CT) DNA (100 μM) in buffer (5 mM Tris/HCl, 50 mM $NaClO_4$, pH = 7.4) was used in order to determine DNA interaction. Stock solutions (5 mM) of each complex in DMSO-H_2O (1:99) with CT DNA were used to achieve molar ratios of 0.1, 0.25, 0.5, 1.0 drug/DNA while keeping a total volume of 3 mL for all compounds. The samples were incubated for 20 h in the dark and maintained at a constant temperature of 37 °C. The CD spectra of DNA-drug adducts and DNA were recorded at a range of 230-340 nm at 25 °C. Noise reduction was performed using the Savitzky–Golay smoothing filter incorporated in the Chirascan software. The spectra are given in molar ellipticity (millidegrees). For the studies under reductive conditions, ascorbic acid (AsA) was used in a one-to-one equivalent (0.25-to-0.25) and glutathione (GSH) in a one-to-two equivalent (0.25-to-0.50) metal-to-reducing agent ratio, while maintaining a 0.25-to-1.0 metal-to-DNA ratio in a total volume of 3 mL.

Thioredoxin Reductase Inhibition assay

$2x10^6$ MDA-MB-231 cells were collected for lysates following a 72-hour dose of IC_{50} or 1 μM concentration of each drug. Lysates were centrifuged and the supernatant containing enzymatic activity was utilized for the assay. The Thioredoxin Reductase Assay Kit (Abcam) was used for measurement of TrxR activity. On ice, samples were pipetted in two sets into a black-bottom 96-well plate. TrxR inhibitor was added to one set of samples to measure background enzyme activity. All of the samples were then reacted with a solution of DTNB and NADPH to determine total DTNB reduction. A standard curve for TNB activity was included. The plate was immediately measured at $OD_{412\ nm}$ to determine baseline activity. After incubating the samples at room temperature with protection from light for 30 minutes, the plate was again measured at OD_{412nm}. TrxR activity inhibition was determined by calculating the difference in activity of samples with and without added inhibitor as a function of time.

Acknowledgements

This research was supported by the National Institute of Health for General Medical Sciences (NIGMS) grant 2SC1GM127278 and R16GM149396-01 (M.C.) and an internship 20596/EE/18 funded by the Fundación Séneca-Agencia de Ciencia y Tecnología de la Región de Murcia (Fundación Séneca – Agency for Science and Technology in the Region of Murcia) under the "Jiménez de la Espada" Regional Program for Researcher Mobility, Cooperation and Internationalization (J.P.C.-C.). I.E.L. thanks the Fulbright Commission/CONICET for a fellowship to conduct research at Brooklyn College. We are grateful to the Brooklyn College Cancer Center (through the Gray Foundation) for a Doctoral Student Mentoring Program award (J.L-H.) during summer 2023. We thank the Graduate Research Technology Initiative Fund Round 21 Supplement from CUNY for funds to purchase a plate reader (M.C). The authors acknowledge the computing resources (the Picasso supercomputer), technical expertise and assistance provided by the SCBI (Supercomputing and Bioinformatics) center of the University of Málaga, a member of the Plataforma Andaluza de Bioinformática.

Conflict of Interest

The authors declare no conflict of interest.

Data Availability Statement

Data available in article Supporting Information.

Keywords: chemotherapeutics • gold(I)-phosphanes heterometallic • platinum(IV) • TNBC

References

[1] G. Housman, S. Byler, S. Heerboth, K. Lapinska, M. Longacre, N. Snyder, S. Sarkar, *Cancers (Basel)* **2014**, 6,1769-1792.

[2] N. White-Al Habeeb, V. Kulasingam, E.P. Diamandis, G.M. Yousef, G.J. Tsongalis, L. Vermeulen, Z. Zhu, S. Kamel-Reid, *Clinical Chemistry*, **2016**, 62,1556–1564.

[3] C. Zhang, C. Xu, X. Gao, Q. Yao, *Theranostics* **2022**, 12, 2115-2132.

[4] R. Oun, Y.E. Moussa, N.J. Wheate, *Dalton Trans*. **2018**, 47, 6645-6653.

[5] K.M. Deo, D.L. Ang, B. BrMcGhie, A. Rajamanickam, A. Dhiman, A.A. Khoury, J. Holland, A. Bjelosevic, B. Pages, C. Gordon, J.R. Aldrich-Wright, *Coord. Chem.* **2018**, 375, 148-163.

[6] J. Zhou, Y. Kang, L. Chen, H. Wang, J. Liu, S. Zeng, L. Yu, *Front. Pharmacol.* **2020**, 11,343.

[7] T.C. Johnstone, K. Suntharalingam, S.J. Lippard, *Chem. Rev.* **2016**, 116, 3436-3486.

[8] R.G. Kenny, C.J. Marmion, *Chem. Rev.* **2019**, 119, 1058-1137.

[9] V. Del Solar, M. Contel, *J. Inorg. Biochem.* **2019**,119, 110780.

[10] S. Rottenberg, C. Disler, P. Perego. *Nat. Rev. Cancer.* **2021**, 21, 37–50.

[11] D.M. Cheff, M.D. Hall, *J. Med. Chem.* **2017**, 60, 4517–4532.

[12] A. Bhargava, U.N. Vaishampayan, *Expert. Opin. Investig. Drugs.* **2009**, 18, 1787-1797.

[13] E. Wexselblatt, D. Gibson, *J. Inorg. Biochem.* **2012**, 117, 220–229.

[14] P. Fronik, M. Gutmann, P. Vician, M. Stojanovic, A. Kastner, P. Heffeter, C. Pirker, B.K. Keppler, W. Berger, C.R. Kowol, *Commun. Chem.* **2022**, 5, 46.

[15] Q. Mi, S.S. Shu, C.X. Yang, C. Gao, X. Zhang, X. Luo, C.H. Bao, X. Zhang, J. Niu, *Clinical Engineering and Radiation Oncology* **2018**, 7, 231-247.

[16] D. Spector, O. Krasnovskaya, K. Pavlov, A. Erofeev, P. Gorelkin, E. Beloglazkina, A. Majouga, *Int. J. Mol. Sci.* **2021**, 22, 3817.

[17] D. Gibson, *J Inorg Biochem.* **2019**, 191, 77–84.

[18] D. Gibson, *J Inorg Biochem.* **2021**, 217, 111353.

[19] L. Ma, L. Li, G. Zhu, *Inorg. Chem. Front.* **2022**, 9, 2424-2453.

[20] L. Ma, R. Ma, Z. Wang, S.M. Yiu, G. Zhu, *Chem. Commun. (Camb).* **2016**, 52,10735-8.

[21] L. Ma, X. Lin, C. Li, Z. Xu, C.Y. Chan, M.K. Tse, P. Shi, G. Zhu, *Inorg Chem.* **2018**, 57, 2917-2924.

[22] L. Shu, L. Ren, Y. Wang, T. Fang, Z. Ye, W. Han, C. Chen, H. Wang, *Chem. Commun. (Camb).* **2020**, 56, 3069-3072.

[23] J. Karges, T. Yempala, M. Tharaud, D. Gibson, G. Gasser, *Angew. Chem. Int. Ed. Engl.* **2020**, 59, 7069-7075.

[24] G. Thiabud, L. Harden-Bull, Y.J. Chang, S. Sen, X. Chi, J.L. Bachman, V.M. Lynch, Z.H. Siddik, J.L. Sessler, *Inorg. Chem.* **2019**, 58, 7886-7894.

[25] K. Yao, G. Karunanithy, A. Howarth, P. Holdship, A.L. Thompson, K.E. Christensen, A.J. Baldwin, S. Faulkner, N.J. Farrer, *Dalton Trans.* **2021,** 50, 8761-8767.

[26] G. Thiabud, G. He, S. Sen, K.A. Shelton, W.B. Baze, L. Segura, J. Alaniz, R.M. Macias, G. Lyness, A.B. Watts, H.M. Kim, H. Lee, M.Y. Cho, K.S. Hong, R. Finch, Z.H. Siddik, J.F. Arambula, J.L. Sessler, *Biological Sciences* 2020,117(13), 7021-7029.

[27] T. Babu, H. Ghareeb, U Basu, H. Schueffl, S. Theiner, P. Heffeter, G. Koellensperger, N. Metanis, V. Gandin, I. Ott, C. Schmidt, D. Gibson, *Angew. Chem. Int. Ed. Engl.* **2023**, 62, e202217233.

[28] Y. Lu, X. Ma, X. Chang, Z. Liang, L. Lv, M. Shan, Q. Lu, Z. Wen, R. Gust, W. Liu, *Chem. Soc. Rev.* **2022**,51, 5518-5556.

[29] S. Yue, M. Luo, H. Liu, S. Wei, *Front. Chem.* **2020**, 8, 543.

[30] F.H. Abdalari, C.M. Telleria, *Discover Oncology* **2021,**12, 42.

[31] N. Curado, M. Contel, in *Metal Based Anticancer Agents*, (Eds: A. Casini, A. Vessieres, S.M. Meier-Menches), Metalobiology Series, Royal Society of Chemistry **2019** ,Ch 6 and refs, therein.

[32] J.E. López-Hernández, M. Contel, *Curr. Opin. Chem. Biol.* **2023** , 72, 102250 and refs, therein.

[33] J. Fernández-Gallardo, B.T. Elie, T. Sadhukha, S. Prabha, M. Sanaú, S.A. Rotenberg, J.W. Ramos, M. Contel, *Chem. Sci.* **2015**, 6, 5269-5283.

[34] B.T. Elie, K. Hubbard, B. Layek, W.S. Yang, S. Prabha, J.W. Ramos, M. Contel, *ACS Pharmacol. Transl. Sci.* **2020**, 3, 644-654.

[35] M. Contel**,** J. Fernández-Gallardo, B.T. Elie, J.W. Ramos, 'Titanocene Gold Derivatives Comprising Thiolato Ligands'. US Patent 9,315,531 (04/19/2016).

[36] B.T. Elie, K. Hubbard, Y. Pechenyy, B. Layek, S. Prabha, M. Contel, *Cancer Med.* **2020**, 8, 4304-4314.

[37] N. Muhammad, N. Sadia, C. Zhu, C. Luo, Z. Guo, X. Wang, *Chem. Commun.* **2017**, 53, 9971–9974.

[38] Z. Wang, Z. Xu, G. Zhu, *Angew. Chem. Int. Ed.* **2016**, 55, 15564–15568.

[39] J.Z. Zhang, P. Bonnitcha, E. Wexselblatt, A.V. Klein, Y. Najajreh, D. Gibson, T.W. Hambley, *Chem. - Eur. J.* **2013**, 19,1672–1676.

[40] Z. Li, Q. Wang, L. Li, Y. Chen, J. Cui, M. Liu, N. Zhang, Z. Liu, J. Han, Z. Wang, *J. Med. Chem.* **2021**, 64, 17920–17935.

[41] J.D. Chai, M. Head-Gordon, *Phys. Chem. Chem. Phys.* **2008**,10, 6615-6620.

[42] V.M. Fernández-Alvarez, S.K.Y. Ho, G.J.P. Britovsek, F. Maseras, *Chem. Sci.* **2018**, 9, 5039-5046.

[43] J.P. Cerón-Carrasco, J. Ruiz, C. Vicente, C. de Haro, D. Bautista, J. Zúñiga, A. Requena, *J. Chem. Theory Comput.* **2017,** 13, 3898-3910.

[44] J.P. Cerón-Carrasco, D. Jacquemin, *ChemPhotoChem* **2017**, 1, 504 – 512.

[45] A. Melchior, J.M. Martínez, R.R. Pappalardo, E. Sánchez Marcos, *J. Chem. Theory Comput.* **2013,** 9, 4562-4573.

[46] F. Weigend, R. Ahlrichs, *Phys. Chem. Chem. Phys.* **2005**, 7, 3297-3305.

[47] G. Moula, M. Bose, S. Sarkar, *New J. Chem.* **2019**, 43, 8332-8340.

[48] M.J. Frisch, G.W. Trucks, H.B. Schlegel, G.E. Scuseria, M.A. Robb, J.R. Cheeseman, G. Scalmani, V. Barone, G.A. Petersson, H. Nakatsuji, X. Li,

M. Caricato, A.V. Marenich, J. Bloino, B.G Janesko, R. Gomperts, B. Mennucci, H.P. Hratchian, J.V. Ortiz, A.F. Izmaylov, J.L. Sonnenberg, D. Williams-Young, F. Ding, F. Lipparini, F. Egidi, J. Goings, B. Peng, A. Petrone, T. Henderson, D. Ranasinghe, V.G. Zakrzewski, J. Gao, N. Rega, G. Zheng, W. Liang, M. Hada, M. Ehara, K. Toyota, R. Fukuda, J. Hasegawa, M. Ishida, T. Nakajima, Y. Honda, O. Kitao, H. Nakai, T. Vreven, K. Throssell, J.A. Jr. Montgomery, J.E. Peralta, F. Ogliaro, M.J. Bearpark, J.J. Heyd, E.N. Brothers, K.N. Kudin, V.N. Staroverov, T.A. Keith, R. Kobayashi, J. Normand, K. Raghavachari, A.P. Rendell, J.C. Burant, S.S. Iyengar, J. Tomasi, M. Cossi, J.M. Millam, M. Klene, C. Adamo, R. Cammi, J.W. Ochterski, R.L. Martin, K. Morokuma, O. Farkas, J.B. Foresman, D.J. Fox, *Gaussian 16* **2016**, Revision A.03, Gaussian, Inc., Wallingford CT.

[49] N. Nayeem, M. Contel, *Eur. Chem*. **2021**, 27, 8891-8917.

[50] L. Ma, L. Li, G. Zhu, *Dalton Trans*. **2022**, 51, 8840.

[51] L.L.Yin, X.M. Wen, Q.H. Lai, J. Li, X.W. Wang, *Oncol. Lett.* **2018**, 5, 6469-6474.

[52] K. Andreidesz, B. Koszegi, D. Kovacs, V. Bagone Vantus, F. Gallyas, K. Kovacs, *Int. J. Mol. Sci.* **2021**; 22, 2056.

[53] U. Olszewski, F. Ach, E. Ulsperger, G. Baumgartner, R. Zeillinger, P. Bednarski, G. Hamilton, *Met. Based. Drugs.* **2009**; 348916.

[54] B.K. Keppler, *Metallomics* **2017**, 9, 309–322.

[55] N. Curado, N. Giménez, K. Miachin, M. Aliaga-Lavrijsen, M.A. Cornejo, A.A. Jarzecki, M. Contel, *ChemMedChem* **2019** 14, 1086-1095.

[56] J. Fernández-Gallardo, B.T. Elie, F.J. Sulzmaier, M. Sanaú, J.W. Ramos, M. Contel, *Organometallics* **2014**, 33, 6669-6681.

[57] B.T. Elie, J. Fernández-Gallardo, N. Curado, M.A. Cornejo, J.W. Ramos, M. Contel, *Eur. J. Med. Chem.* **2019**, 161, 310-322.

[58] B.T. Elie, Y. Pechenyy, F. Uddin, M. Contel, *J. Biol. Inorg. Chem.* **2018**, 23, 399-411.

[59] S. Elmore *Toxicol. Pathol.* **2007**, 4, 495-516.

[60] K. Andreidesz, B. Koszegi, D. Kovacs, V. Bagone Vantus, F. Gallyas, K. Kovacs, *Int. J. Mol. Sci.* **2021,** 22, 2056.

[61] L. Agnello, S. Tortorella, A. d'Argenio, C. Carbone, S. Camorani, E. Locatelli, L. Auletta, D. Sorrentino, M. Fedele, A. Zannetti, M.C. Franchini, L. Cerchia, *J. Exp. Clin. Cancer Res.* **2021**, 40, 239.

[62] Y. Guo, S. Zhang, H. Yuan, D. Song, S. Jin, Z. Guo, X. Wang, *Dalton Trans.* 2019, **48**, 3571– 3575.

[63] N. Muhammad, C.-P. Tan, U. Nawaz, J. Wang, F.-X. Wang, S. Nasreen, L.-N. Ji, Z.-W. Mao, *Inorg. Chem.* **2020**, 59, 12632– 12642.

[64] C. Yang, K. Tu, H. Gao, L. Zhang, Y. Sun, T. Yang, L. Kong, D. Ouyang, Z. Zhang, *Biomaterials* **2020**, 232, 119751.

[65] S. Moens, P. Zhao, M.F. Baietti, O. Marinelli, D. Van Haver, F. Impens, G. Floris, E. Marangoni, P. Neven, D. Annibali, A.A. Sablina, F. Amant, *Sci. Rep.* **2021**,11, 3176.

[66] T. Tippayamontri, R. Kotb, B. Paquette, L. Sanche, *Invest. New Drugs.* **2011**, 29, 1321-1327.

[67] C.I. Yeo, K.K. Ooi, E.R.T. Tiekink. *Molecules* **2018**, 23, 1410.

[68] A. Sigel, H. Sigel, E. Freisinger, R.K.O Sigel, *Metallo-Drugs: Development and Action of Anticancer Agents*, Berlin, Boston: De Gruyter, **2018**.

[69] C.C. Liang, A.Y. Park, J.L.Guan, *Nat. Protoc.* **2007**, 2,329-333.

[70] Z.-Y. Ma, D.-B. Wang, X.-Q. Song, Y.-G. Wu, Q. Chen, C.-L. Zhao, J.-Y. Li, S.-H. Cheng, J.-Y. Xu, *Eur. J. Med. Chem.* **2018**, 157, 1292– 1299.

[71] R. Kapoor, V. Reddy, P. Kapoor, *Bioscience Solutions Lonza,* **2017.**

[72] W. Zhang, K. Kai, N.T. Ueno, L. Qin, *Cancer Hallm.* **2013**, 1, 59-66.

[73] K.L. DeCicco-Skinner, G.H. Henry, C. Cataisson, T. Tabib, J.C. Gwilliam, N.J. Watson, E.M. Bullwinkle, L. Falkenburg, R.C. O'Neill, A. Morin, J.S. Wiest. *J. Vis. Exp.* **2014,** 91, e51312.

[74] C. Jensen, Y. Teng, *Front Mol Biosci.* **2020**, 7, 33.

[75] S.A. Langhans, *Front Pharmacol.* **2018** 9, 6.

[76] S. Breslin, L. O'Driscoll, *Oncotarget* **2016,** 7, 45745-45756.

[77] A.M. Heijink, M. Everts, M.E. Honeywell, R. Richards, Y.P. Kok, E.G.E. de Vries, M.J. Lee, M.A.T.M. van Vugt, *Cell Rep.* **2019**, 28, 2345-2357.

[78] M. Muguruma, S. Teraoka, K. Miyahara, A. Ueda, M. Asaoka, M. Okazaki, T. Kawate, M. Kuroda, Y. Miyagi, T. Ishikawa, *Biochem Biophys Res Commun.* **2020**, 533, 268-274.

[79] L. Massai, J. Fernández-Gallardo, A. Guerri, A. Arcangeli, S. Pillozzi, M. Contel, L. Messori, *Dalton Trans.* **2015**, 44, 11067-11076.

[80] M. Frik, J. Fernández-Gallardo, O. Gonzalo, V. Mangas-Sanjuan, M. González-Alvarez, A. Serrano del Valle, C. Hu, I. González-Alvarez, M. Bermejo, I. Marzo, M. Contel, *J. Med. Chem.* **2015**, 58, 5825-5841.

[81] J. Fernández-Gallardo, B.T. Elie, M. Sanaú, M. Contel, *Chem. Commun. (Camb).* **2016,** 5, 3155-3158.

[82] Y. Shi, S.A. Liu, D.J. Kerwood, J. Goodisman, J.C. Dabrowia, *J. Inorg. Biochem.* **2012**, 107, 6-14.

[83] D. Wragg, A. de Almeida, R. Bonsignore, F.E. Kühn, S. Leoni, A. Casini, *Angew. Chem. Int. Ed. Engl.* **2018**, 57,14524-14528.

[84] S. Zhang, H. Yuan, Y. Guo, K. Wang, X. Wang, Z. Guo, *Chem. Commun.* **2018**, 54, 11717– 11720.

[85] C.K. Chen, J.Z. Zhan, J.B. Aitken, T.W. Hambley, *J. Med. Chem.* **2013**, 56, 8757-8764.

[86] J.Z. Zhang, E. Wexselblatt, T.W. Hambley, D. Gibson, *Chem. Commun. (Camb).* **2012**, 6, 847-849.

[87] M.P. Rigobel, L. Messori, G. Marcon, M. Agostina Cinellu, M. Bragadin, A. Folda, G. Scutari, A. Bindoli, *J. Inorg. Biochem.* **2004**, 98, 1634-1641.

10.1002/chem.202302045

WILEY-VCH

RESEARCH ARTICLE

Table of Contents

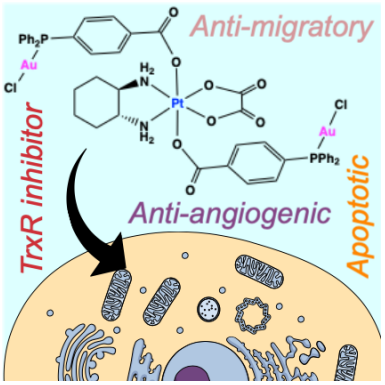

Two better than one, heterometallic anticancer agents continue to impress: A Platinum(IV)-gold(I) agent inhibits several TNBC cancer hallmarks with no decreased drug sensitivity in 3D spheroids versus 2D cell culture models, inhibiting thioredoxin reductase (TrxR) enzyme in cells at concentrations five-times lower than IC_{50} value.

Institute and/or researcher Twitter usernames: (@ContelLab)(@javoed_)(@naznayeem)(@AfrujaAhad)(@jpcer0n)(@IgnacioELeon)